

## **SYMMETRIC AND ASYMMETRIC DOUBLE LANGMUIR PROBES CHARACTERIZATION OF RADIO FREQUENCY INDUCTIVELY COUPLED NITROGEN PLASMA**

**M. Y. Naz and A. Ghaffar**

Department of Physics  
University of Agriculture Faisalabad, Pakistan

**N. U. Rehman**

Department of Physics  
COMSATS Institute of Information Technology, Islamabad, Pakistan

**M. Azam and S. Shukrullah**

Department of Physics  
University of Agriculture Faisalabad, Pakistan

**A. Qayyum**

Pakistan Institute of Nuclear Science and Technology  
Islamabad, Pakistan

**M. Zakaullah**

Departments of Physics  
Quaid-I-Azam University, Islamabad 45320, Pakistan

**Abstract**—The symmetric and asymmetric double Langmuir probe systems with their necessary driving circuits are developed for characterization of low pressure inductively coupled nitrogen plasma, generated and sustained with 13.56 MHz RF source and an automatic impedance matching network. First of all, the plasma parameters such as ion saturation current, electron temperature and electron number density are determined with symmetric double probe system at different input RF powers, filling gas pressures and radial distance

from the plasma chamber wall. Then the electron temperature and electron energy probability function are determined with asymmetric double probe system at the centre of the discharge plasma chamber by changing the filling gas pressure and input RF power. It is observed that the electron temperature and electron number density increase with the increase in input RF power and radial distance but decreases with the increase in filling gas pressure. The electron energy probability function determined with asymmetric probe system evidently deviates from the Maxwellian, particularly at low filling gas pressures.

## 1. INTRODUCTION

The low pressure inductively coupled plasmas (ICPs) have non-local thermodynamical behavior which shows that a number of non-equilibrium conditions might be possible physically and chemically by changing the working discharge gas, electrode configuration, filling gas pressure, externally imposed electromagnetic field structure, input power and discharge plasma volume [1].

Different power sources can be used to generate and sustain the low pressure discharge plasmas and ICP source is one of them. The low pressure ICPs have tremendous scope in discharge plasma processing industry. The generation and characterization of plasma discharges of molecular gases like: nitrogen, oxygen, chlorine and methane or their mixture with others gases have wide range of applications in material processing. Thin film deposition, etching, nitriding of metals and alloys and surface treatment of polymers are most common examples of material processing. In response to nitriding, the substrate surface properties like: metallic strength, hardness, wearing and tearing and corrosion resistance show great improvement. In ICPs, the electron temperature ( $kT_e$ ) and electron number density ( $n_e$ ) are much important parameters to understand the processes like electron impact ionization and excitation [1]. As the rate of thin film deposition is determined by the degree of ionization and  $n_e$  which depend on  $kT_e$  and electron energy distribution function (EEDF) [2]. It shows that discharge plasma processing of different materials depends upon plasma parameters and therefore it is important to determine these parameters in a very precise way [3].

The phenomena of low pressure gas discharges becomes very complex during the conversion of electron energy into some other forms such as chemical energy, sound energy, light energy and heat. In ICPs the electrons are of great importance and play a vital role in transportation of energy within the plasma volume. They have

frequent collisions with each other and with other plasma species and remain in an equilibrium state with a definite EEDF and electron energy probability function (EEPF) [1]. For the Maxwellian energy distribution, the semi logarithmic plot of EEPF is a straight line which shows that it is much importance and simpler to analyse in comparison with corresponding EEDF. In high density low pressure plasma discharges, the knowledge of plasma potential ( $V_p$ ),  $kT_e$ ,  $n_e$ , EEDF, and EEPF at different locations and input plasma parameters is much important in discharge plasma processing of different materials.

Different tools and techniques are available to fully characterize these low pressure discharge plasmas over a wide range of electron temperatures and electron numbers densities. The optical emission spectroscopy and Langmuir probes are most commonly used techniques for discharge plasma characterization. In optical emission spectroscopy technique, we can diagnose the excited energy states of particles instead of electrons by their emissions spectrum [4]. On the other hand the Langmuir probes can diagnose the electron energy states in non-LTE discharge plasmas and corresponding EEDF and EEPF can be determined from their I-V characteristics curve. During the plasma characterization, the single Langmuir probes (SLPs) encounter some problems particularly when the reference electrode is not there or when the discharge plasma potential is not well defined. Moreover, when SLPs are operated close to space potential, they might disturb the plasma by drawing large electronic currents. It shows that the SLPs are not suitable to characterize the decaying plasmas accompanied by the perturbations. All these difficulties introduced by SLPs can be overcome by introducing symmetric and asymmetric double Langmuir probes. These probes yield an accurate data for determination of discharge plasma parameters with negligible influence on discharge plasmas [4].

In our previous work [1], symmetric double and triple Langmuir probes were developed along with their necessary driving circuits to characterize ICP powered with 13.56 MHz RF source. The discharge plasma parameters such as  $kT_e$ ,  $n_e$  [5] and  $I_{io}$  were evaluated as the function of input plasma parameters. In the present work which is an extension of our previous work, DC biased symmetric and asymmetric double Langmuir probes [6, 7] are developed along with their necessary driving circuits. These probes are used to investigate 13.56 MHz RF inductively coupled nitrogen plasma to check its suitability for material processing. The nitrogen discharge plasma parameters such as  $kT_e$ ,  $n_e$ ,  $I_{io}$  and EEPF are evaluated as the function of changing input plasma parameters like: working gas pressure, input RF power, gas flow rate and radial distance within the discharge plasma chamber.

## 2. PRINCIPLE OF DIAGNOSTIC TOOLS

### 2.1. Symmetric Double Probe

A symmetric double probe method (DPM) consists of a pair of SLPs of same geometrical shape and size. A variable DC biasing source is connected across these small probes with an associated current through the circuit as shown in the Figure 1. If the electrons in discharge plasma obey the Maxwellian energy distribution, then the plasma parameters can be evaluated from the I-V characteristics curve of double probe using the equation given below [1, 5, 6]:

$$\left(\frac{dI}{dV_d}\right)_{V_d=0} = eI_{io}/2kT_e \quad (1)$$

The above equation shows that the slope of I-V characteristics curve at zero relative DC bias voltage provides the  $kT_e$  and  $I_{io}$ . Then  $n_e$  can be determined from the  $I_{io}$  and  $kT_e$  by using the following equation:

$$I_{io} = 0.61n_e e A_p \sqrt{kT_e/m_i} \quad (2)$$

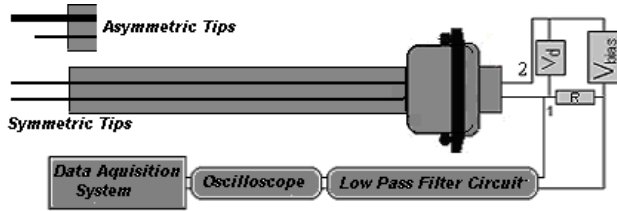


**Figure 1.** A schematic diagram of double Langmuir probe system.

While we were determining the  $kT_e$  from the I-V characteristics curve of symmetric DPM, it was assumed that the high energy electrons obey the Maxwellian distribution to overcome the retarding field of probes. But it is observed that the most of discharge plasmas obey the non-Maxwellian energy distribution and the symmetric DPM gives more erroneous data during the characterization of these plasmas [4].

### 2.2. Asymmetric Double Probe

As the electrons collected by the symmetric double probe comes from the high energy tail of the EEDP. Therefore, the electrons in these types of discharge plasmas have Maxwellian distribution and the  $kT_e$  determined by symmetric DPM shows close agreement with the measurements made with SLP method which has ability to scan the

full energy range. Hence, it is possible to determine the EEDF and EEPF only with SLP method but not with symmetric DPM. This small discrepancy can be overcome by changing the symmetry of double probes. For the collection of majority of electrons by the probe from the whole energy distribution, the area of the one probe is increased several hundred of times than the other one. Then the EEDF can be determined by taking the second derivative of electron current ( $I_e$ ) w. r. t. repelling potential given as [4]:

$$F_e(\varepsilon) = \frac{4}{A_p e^2} \sqrt{m_e V / 2e} \frac{d^2 I_e}{dV^2} \quad (3)$$

In this equation,  $\varepsilon = eV = e(V_p - V_s)$  is the electron energy,  $I_e = I_p - I_{io}$  is the electron current,  $m_e$  is the electron mass,  $A_p$  is the probe area,  $V_s$  is the space potential and  $I_p$  is the probe current. If the plasma electrons have the Maxwellian energy distribution, the log plot of EEPF will be a straight line which shows that EEPF is easier to analyze than the corresponding EEDF. Hence, using equation-3 we can determine the EEPF as:

$$F_p(\varepsilon) = \varepsilon^{-1/2} F_e(\varepsilon) \quad (4)$$

The average electron energy or electron temperature which is also called effective electron temperature can be determined by the equation given below:

$$\langle \varepsilon \rangle = \frac{3}{2} kT_e \quad (5)$$

$$kT_e = \frac{2}{3} \langle \varepsilon \rangle \quad (6)$$

The asymmetric DPM can not be used to determine  $n_e$  in the plasmas having non-Maxwellian EEDF.

### 3. EXPERIMENTAL SETUP

The schematic diagram of experimental setup used for generation and characterization of inductively coupled nitrogen plasma is shown in Figure 2 [1]. It consists of a set of different components. The nitrogen plasma is generated and sustained with 13.56 MHz RF source having  $50 \Omega$  resistance [5–8]. This RF source is connected across a water cooled spiral planar coil shaped electrode. The copper electrode has total 13 turns with 30 cm diameter and is placed at the top opening of cylindrical plasma chamber. This stainless steel plasma chamber is 24 cm in height and 30 cm in diameter with four multi purpose ports. A 1.2 cm thick quartz plate is used at the top opening of

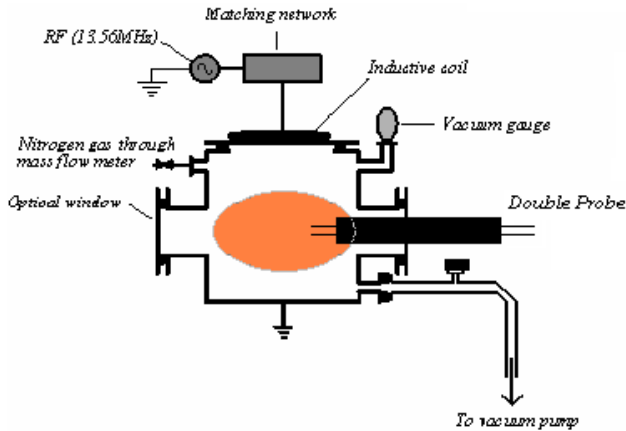


**Figure 2.** A schematic diagram of experimental setup.

the chamber to insulate the water cooled spiral planar coil from the plasma chamber [9, 10]. The quartz plate, not only insulate the coil electrode from the plasma chamber but also helps in making the plasma chamber vacuum tight. During the plasma generation, the reflected power is kept below 2% by an automatic impedance matching network consisting of a control unit and a tuning unit. This matching network is always connected between RF source and spiral planar coil to minimize the power reflection and to maximize the power transfer from the RF source to discharge plasma in the chamber. For low pressure discharge plasma generation and flow mode operation, the plasma chamber is employed with a rotary vane pump which has the ability to lower the gas pressure upto  $10^{-3}$  mbar. In order to monitor the pressure inside the chamber, a pirani gauge is used while the gas flow rate from the main cylinder to plasma chamber is monitored with mass flow meter. The nitrogen gas flow rate is kept constant at 50 sccm throughout the current experiment.

### 3.1. Development of Symmetric and Asymmetric Double Probes

The careful manufacturing and electric circuit design is much important for successful use of symmetric and asymmetric double probes for plasma characterization. To verify the compatibility of the probe dimensions chosen for particular experiment, the probe theory presented in this paper must be applicable during the evaluation of expected discharge plasma parameters. Keeping this in mind, the

symmetric and asymmetric double probe systems are developed in the laboratory to diagnose the inductively coupled nitrogen discharge plasma shown in the Figure 2. The symmetric double probe consists of two plasma exposed Nickel-Chrome tips of same length, radius and surface area. These tips are 0.11 mm in radius and 11 mm in length with surface area of  $7.59 \text{ mm}^2$ .

The asymmetric double probe also comprises of two plasma exposed tips of same material but not of same dimensions as in the case of symmetric double probe. One of the exposed tips has the area  $2.76 \text{ mm}^2$  while the 2nd tip area is  $261.25 \text{ mm}^2$ . Both of these probes are connected to BNC coaxial cables running along the probe arm and down to an insulated BNC feed through [11, 12]. These coaxial cables pass the electrical signal out of the plasma chamber to the digital oscilloscope via circuit arrangements made for these probes. A DC biasing source (+120 V to -120 V) is connected across the probe for manual scanning from +26 V to -26 V and corresponding current through the probe circuit is measured [13, 14]. For the elimination of RF noise picked up by data cables, the RC low pass filters are used at the inputs of the oscilloscope and a single common ground is provided to the entire experimental setup.

#### 4. EXPERIMENTAL MEASUREMENTS

The I-V characteristics curve of symmetric double probe at 300 W input RF power [14, 15] and 0.3 mbar filling gas pressure is shown in the Figure 3. The  $kT_e$  and  $I_{io}$  at different input powers (300, 350, 400, 450 W), filling gas pressures (0.3, 0.4, 0.5, 0.6 mbar) and the radial positions (4, 6, 8, 10, 12, 14 cm) of symmetric double probe from the discharge plasma chamber wall are determined from the slope of the I-V characteristics curve and Equation (1). Then using these values of  $kT_e$  and  $I_{io}$  in Equation (2), we can determine the  $n_e$ . The currents from the discharge plasma to probes might be due to convection, diffusion, high energy electrons in the tail of EEDF and electric field of sheath around the probes [1, 16]. It predicts that for accurate measurements of plasma parameters from the characteristics curve, the Equation (1) should be satisfied. So a necessary correction in the I-V characteristics curve is done by fitting a straight line to the ion saturation regime of the curve as shown by red line in the Figure 3.

The typical I-V characteristics curve for asymmetric double probe at 300 W input RF power, 0.3 mbar pressure and 14 cm far from the wall is shown in the Figure 4. As the asymmetric double probe tips receive the different electron flux, the characteristics curve does not pass through the origin of the co-ordinate system. From this I-V

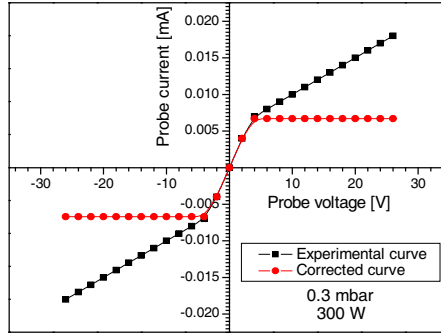


**Figure 3.** The experimental and corrected I-V characteristics curve at 300 W RF power and 0.3 mbar filling gas pressure.

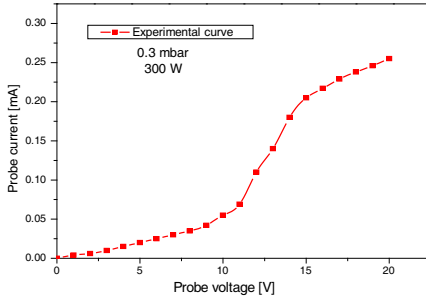


**Figure 4.** I-V characteristics curve of asymmetric double probe at 300 W RF power and 0.3 mbar filling pressures.

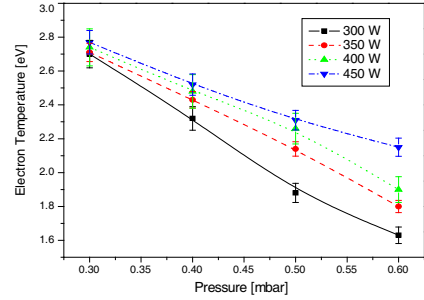


**Figure 5.** The electron temperature determined with symmetric double probe method at different filling gas pressures and input RF powers.

characteristics curve, the  $I_{io}$  can be determined in similar way to the single Langmuir probe. The turning point of this curve gives the space potential which is used along with  $I_{io}$  to determine the electron current ( $I_e = I_p - I_{io}$ ) and repelling potential ( $V = V_s - V_p$ ). Then putting these parameters in Equations (4), (5), (6), we can easily evaluate the EEPF,  $\langle \varepsilon \rangle$  and  $kT_e$ . The measurements with asymmetric double probe are carried out at different filling gas pressures and input RF powers while keeping its radial position fix at 14 cm from the wall.

### 5. RESULTS AND DISCUSSION

The graphical representation of  $kT_e$  obtained with the symmetric and asymmetric DPM at different filling gas pressures and input RF powers is shown in the Figures 5 & 6. The  $kT_e$  is an important discharge plasma parameter which not only controls the production of active species via collisional process but also determines the rate process of the reactive gases in discharge plasmas. So it is imperative to regulate the plasma electron temperature to control the selected process according to the requirements. Therefore, the experimental measurements show that the  $kT_e$  increases with the increase in input RF power from 300 to 450 W and decreases with the increase in filling gas pressure from 0.3 to 0.6 mbar [1, 17]. This increasing trend in  $kT_e$  with input RF power may be due to an increase in kinetic energy of electrons under the influence of rising incident RF power. Another important factor for increase in  $kT_e$  with power is that at low pressure and high input RF power, the electron collision probability decreases by providing sufficient time and mean free path for electrons to be accelerated which results in an increase of  $kT_e$ . However, the most important reason could be the availability of more and more energetic electrons in the high energy tail of the EEDF at higher input powers.

The decreasing trend in  $kT_e$  with increase in filling gas pressure may be due to the following reasons: The increasing gas pressure inside the discharge plasma chamber brings about high cooling frequency which results in decrease of average electron energy and consequently

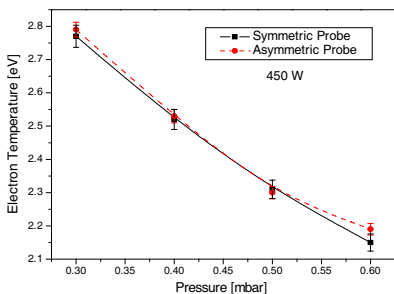


**Figure 6.** The electron temperature determined with symmetric and asymmetric double probe methods at 450 W input RF power and different filling gas pressures.

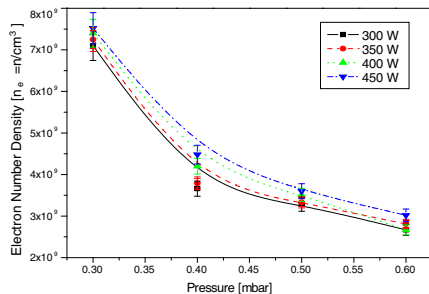


**Figure 7.** The electron number density determined with symmetric double probe method at different filling gas pressures and input RF powers.

the  $kT_e$  [1, 17]. The filling gas pressure dependence of average electron energy can also be expressed by the steady state particle balance equation. As there is a linear relationship between the effective electron temperature and average electron energy, the increase in filling gas pressure also causes an increase in electron collision frequency with the discharge plasma species. It shows that rather an increase in electron energy, more and more energy transfer from electrons to the discharge plasma species takes place. Under these conditions the  $kT_e$  decreases and neutral gas temperature increases due to the existence of a balance between the total ionization events and the total particle losses to the plasma chamber walls [7, 18]. The particle-wall recombination probability is different for different wall surfaces. It depends upon the wall roughness, crystal structure, incoming particle's state and contamination of walls and discharge plasmas. According to Kim and Boudart, the particle-wall recombination probability varies from  $1 \times 10^{-5}$  to  $1 \times 10^{-3}$  for hydrogen and  $2 \times 10^{-6}$  to  $2 \times 10^{-4}$  for nitrogen [19]. It shows that most of the energetic particles formed in these reactions go back to their ground state or diffuse to the walls by collisions with themselves or with other particles. While determining the  $kT_e$  with symmetric DPM, it was assumed that the high energy electrons obey the Maxwellian energy distribution. It predicts that the values of  $kT_e$  obtained by symmetric DPM should be some what higher that obtained by asymmetric DPM. But in this experiment, the measurements for  $kT_e$  with both methods show close agreement and confirms the non-Maxwellian nature of discharge plasma as shown in Figure 6.

The variational trend of  $n_e$  with changing input RF power and filling gas pressure is shown in Figure 7. It is clear from the graph that the  $n_e$  increases with increase in RF power and decreases with increase in filling gas pressure. Although, the  $n_e$  has inverse relation with  $kT_e$  as mentioned earlier in double probe theory, but in this experiment it increases proportionally with the  $kT_e$  as the input RF power moves to higher values. This rise in  $n_e$  may be due to an increase in ionization events within the plasma and hence the  $I_{io}$ . The  $I_{io}$  has direct relationship with the  $n_e$  and justifies the observed increment in  $n_e$  [17]. The increment in ionization events can be explained as; the rising input RF power makes available more and more energy to be transferred to the discharge plasma and results in high ionization probabilities particularly at low filling gas pressures.

The decreasing trend of  $n_e$  with filling gas pressure can be explained as follow: The rise in filling gas pressure inside the discharge plasma chamber gives a cooling affect in plasma. This cooling affect in plasma decreases the  $I_{io}$  and consequently the  $n_e$  [1, 20]. At low input

RF powers and relatively high filling gas pressures, the elastic collisions of electrons with discharge plasma species dominates and also play key role in reduction of ionization events. The increasing pressure also depletes the high energy tail of the EEDF to the lower energies and decreases the availability of high energy electron for electron impact ionization processes and consequently the  $n_e$ . The depletion in the high energy tail of EEDF might be due to rapid recombinations and diffusion of high energy electrons to the walls of the plasma chamber [1, 20].

The  $kT_e$  and  $n_e$  obtained with symmetric DPM at 450 W input RF power, 0.3 mbar filling gas pressure and different radial positions from the plasma chamber wall is shown in Figures 8 & 9. It is observed that  $kT_e$  and  $n_e$  increase with the increase in radial distance. When the probe is located close to the centre of discharge plasma chamber, it can collect many electrons particularly at low pressures. As the electron flux in this region is strong and high energy electrons can easily reach the probe without having significant collisions with other plasma species. During the measurements with symmetric DPM, the electrons collected by the probe were supposed to come from the high energy tail of the EEDF. As the probe moves toward the centre of the plasma chamber, the electron flux starts increasing and consequently the high energy electrons and  $kT_e$ . The high energy electron flux at the centre is due to the resonantly enhanced electric field and the local plasma frequency in this region becomes equal to the applied frequency. The increase in  $n_e$  with the radial distance is due to the increase in  $I_{i0}$  measured from the I-V characteristics curve [21].

The EEPF is more easy to analyze than corresponding EEDF, determined with asymmetric DPM at 0.3, 0.4, 0.5 mbar filling gas

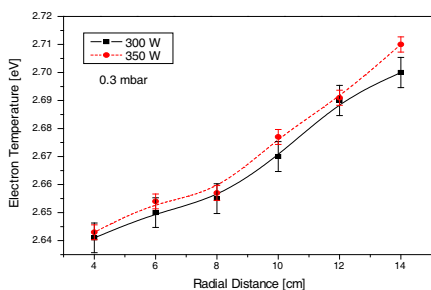


**Figure 8.** The electron temperature determined with symmetric double probe method at different radial positions and input RF powers.

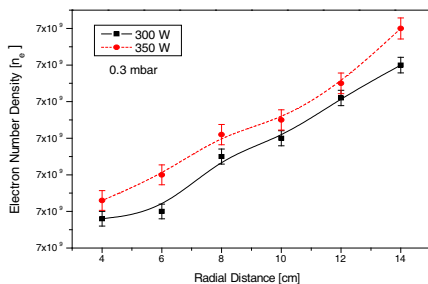


**Figure 9.** The electron number density determined with symmetric double probe method at different radial positions and input RF powers.

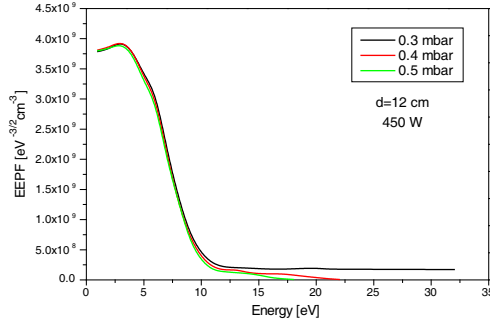


**Figure 10.** EPPFs determined with asymmetric double probe at 450 W input RF power and different filling gas pressures.

pressures and 450 W input RF power as shown in Figure 10. It is clear from the figure that the high energy tail of EPPF increases with the decrease in filling gas pressure, showing its non-Maxwellian behavior. This increment in the tail confirms the presence of large number of highly energetic electrons in the discharge plasma [18] along with the least energetic electrons. But at higher pressures the high energy tail of the EPPF depletes to the lower energies, indicating the Maxwellian approach of EPPF. This depletion in high energy tail may be due to the rapid diffusion and recombinations of high energy electrons at the chamber walls. The electrons have random motion and undergo inelastic collisions with plasma species. During these collisions, they exchange their energies with other particles, resulting in reduction of fast electrons near the probes and consequently the high energy tail [1, 4].

Although, the double Langmuir probes are very good tools for discharge plasma characterization but they have some major drawbacks. As they measure only the highly energetic electrons in the tail of the EEDF, these electrons take only a little influence of the probe electric field at relatively small biasing voltages and cause an inaccuracy in measurements in retardation region which can normally range from 10% to 25%. To overcome this problem a sensitive driving circuit is required for double probes [22] which not only makes them more complicated and susceptible to disturbances in the discharge plasma but also causes the grounding problems. Another serious problem faced by the double Langmuir probes, is the investigation of electronegative discharge plasmas for material processing. In these plasmas the negative ion number density is usually higher than the electron number density particularly at low input RF powers and high filling gas pressures.

## 6. CONCLUSION

The double Langmuir probes work very well even in the situations, where the probe tips are deposited in real discharge plasma processing of materials. So keeping this in mind, the symmetric and asymmetric double Langmuir probes along with their necessary driving circuits are developed successfully to determine the low pressure inductively coupled nitrogen plasma parameters like: ion saturation current, electron temperature, electrons number density and electron energy probability function at different values of input RF power, filling gas pressure and radial distance from the chamber wall. First the electron temperature and electron number density are determined with the symmetric double probe method at filling gas pressure ranging from 0.3 to 0.6 mbar, input RF power ranging from 300 to 450 W and radial distance ranging from 4 to 14 cm. It is observed that the electron temperature and electron number density increase with the increase in input RF power and radial distance from the wall but decreases with the increase in filling gas pressure.

Then the electron temperature and the electron energy probability function are determined with asymmetric double probe method at 450 W input RF power and 0.3, 0.4, 0.5, 0.6 mbar filling gas pressure. It is observed that the electron temperature determined with asymmetric double probe method shows a close agreement with that determined with symmetric double probe method. As for as the determination of electron energy probability function is concerned, it is observed that the high energy tail of the electron energy probability function shrinks to the lower energies with the increase in filling gas pressure. It confirms the non-Maxwellian nature of the electron energy probability function and presence of two groups of the energetic electrons at low pressures. The final outcomes of the present experiment show that the modifications in discharge plasma parameters strongly depend upon the input parameters which could be helpful for tuning the operating conditions in nitrogen discharge plasmas processing of specific materials.

## REFERENCES

1. Naz, M. Y., A. Ghaffar, N. U. Rehman, S. Naseer and M. Zakaullah, "Double and triple Langmuir probes measurements in inductively coupled nitrogen plasma," *Progress In Electromagnetic Research*, Vol. 114, 113–128, 2011.
2. Jain, R. and M. V. Kartikeyan, "Design of a 60 GHz, 100 kW CW

- gyrotron for plasma diagnostics: GDS-V.01 simulations,” *Progress In Electromagnetics Research B*, Vol. 22, 379–399, 2010.
3. Singh, S. B., N. Chand, and D. S. Patil, “Langmuir probe diagnostics of microwave electron cyclotron resonance (ECR) plasma,” *Elsevier*, Vol. 83, 372–377, 2009.
  4. Ling, Y.-M., “Probe diagnosis of electron temperature and electron energy distribution in low-pressure dielectric discharge,” *Physics of Plasmas*, Vol. 12, 113504, 2005.
  5. Pandey, R. S. and R. P. Pandey, “Cold plasma injection on VLF wave mode for relativistic magnetoplasma with A.C. electric field,” *Progress In Electromagnetics Research C*, Vol. 2, 217–232, 2008.
  6. Manory, R. R., U. Carmi, R. Avni, and A. Grill, “A comparative study of silicon deposition from SiCl<sub>4</sub> in cold plasma using argon, H<sub>2</sub> or Ar + H<sub>2</sub>,” *Thin Solid Films*, Vol. 156, 1988.
  7. Pandey, R. S. and D. K. Singh, “Study of electromagnetic ion-cyclotron instability in a magnetoplasma,” *Progress In Electromagnetics Research M*, Vol. 14, 147–161, 2010.
  8. Sha, W. E. I. and W. C. Chew, “High frequency scattering by an impenetrable sphere,” *Progress In Electromagnetics Research*, Vol. 97, 291–325, 2009.
  9. Costa, E. M. M., “Parasitic capacitances on planar coil,” *Journal of Electromagnetic Waves and Applications*, Vol. 23, No. 17–18, 2339–2350, 2009.
  10. Wen, S. and L. Zhu, “Numerical synthesis design of coupled resonator filters,” *Progress In Electromagnetics Research*, Vol. 92, 333–346, 2009.
  11. Jian, L. and K. T. Chau, “Analytical calculation of magnetic field distribution in coaxial magnetic gears,” *Progress In Electromagnetics Research*, Vol. 92, 1–16, 2009.
  12. Shiri, A. and A. Shoulaie, “A new methodology for magnetic force calculations between planar spiral coils,” *Progress In Electromagnetics Research*, Vol. 95, 39–57, 2009.
  13. Wu, H. W. and R. Y. Yang, “Design of a triple-passband microstrip bandpass filter with compact size,” *Journal of Electromagnetic Waves and Applications*, Vol. 24, No. 17–18, 2333–2341, 2010.
  14. Pandey, R. S., “Gradient effect on kelvin helmholtz instability in the presence of inhomogeneous d.c. electric field,” *Progress In Electromagnetics Research B*, Vol. 11, 39–53, 2009.
  15. Ibrahiem, A., C. Dale, W. Tabbara, and J. Wiart, “Analysis of the

- temperature increase linked to the power induced by RF source,” *Progress In Electromagnetics Research*, Vol. 52, 23–46, 2005.
16. Rossnagel, S. M., R. J. Cuomo, and W. D. Westwood, “Handbook of plasma processing technology,” *Noyes Publications*, Park Ridge, NJ, 1910.
  17. Yong-ik, S., H. B. Lim, and R. S. Houk, “Diagnostic studies of low-pressure inductively coupled plasma in argon using a double Langmuir probe,” *J. Anal. At. Spectrom.*, Vol. 17, 565–569, 2002.
  18. Pu, Y. K., Z. G. Guo, A. U. Rehman, and Z. D. Yu, “Tuning effect of inert gas mixing on electron energy distribution function in inductively coupled discharges,” *Ma. J. Plasma Phys. and Control. Fusion*, Vol. 48, 2006.
  19. Khan, F. U., N. U. Rehman, S. Naseer, M. A. Naveed, A. Qayyum, N. A. D. Khattak, and M. Zakaullah, “Diagnostic of 13.56 MHz RF sustained Ar-N<sub>2</sub> plasma by optical emission spectroscopy,” *J. Appl. Phys.*, Vol. 45, 11002, 2009.
  20. Yin, Q., L. S. Wu, L. Zhou, and W. Y. Yin, “Compact dual-band bandpass filter using asymmetrical dual stub-loaded open loops,” *Journal of Electromagnetic Waves and Applications*, Vol. 24, No. 17–18, 2397–2406, 2010.
  21. Husarik, J., M. Siry, and M. Kando, “Double probe characteristics in high-energy electron flux pressure,” *J. Appl. Phys.*, Vol. 47, 7334–7338, 2008.
  22. Xia, Q., Z. X. Tang, and B. Zhang, “A Ku-band push-push dielectric resonator oscillator,” *Journal of Electromagnetic Waves and Applications*, Vol. 24, No. 14–15, 1859–1866, 2010.